Snap-Off of Gas Bubbles in Smoothly Constricted Noncircular Capillaries

A corner flow hydrodynamic theory is outlined for the time to snap-off of a gas bubble moving through a smoothly constricted noncircular capillary as a function of the pore geometry and the capillary number, *Ca*. Above a transition capillary number the time to snap-off is independent of *Ca*, while below it the time to snap-off is inversely proportional to the capillary number. Thin films of liquid deposited along the capillary walls are shown to play a minor role; they are accordingly neglected in the analysis. The proposed theory is compared to new experimental results for snap-off in two constricted square capillaries (dimensionless constriction radii of 0.3 and 0.5) over a range of capillary numbers (10^{-5} to 10^{-3}), wetting-liquid viscosities (1.0 to 8.5 mPa · s), and surfactant types. Good agreement is found between theory and experiment.

T. C. Ransohoff, P. A. Gauglitz
C. J. Radke
Department of Chemical Engineering
University of California, Berkeley
Berkeley, CA 94720

Introduction

An understanding of the foam generation process in porous media is important to foam flooding as an enhanced oil recovery technique (Fried, 1961) and to foaming in trickle-bed reactors (Charpentier and Favier, 1975). One of the primary mechanisms of foam generation in porous media is the snap-off of gas bubbles passing through constricted pores (Mast, 1972; Ransohoff and Radke, 1986a). Most flow channels in porous media are noncircular in cross section (Dullien, 1979), and a difference in the effect of gas-bubble velocity on snap-off in constricted circular and noncircular capillaries has been demonstrated experimentally (Gauglitz, 1986). Therefore, it is important to understand and model the snap-off process in a constricted noncircular pore. Although the problem of snap-off in cylindrical capillaries has been thoroughly studied (Gauglitz, 1986; Goren, 1962; Hammond, 1983), little effort has been directed toward gas-bubble breakup in noncircular capillaries.

Work related to snap-off in noncircular pores has been presented by a number of authors. Lenormand and Zarcone (1984) identified snap-off as one of the processes involved in two-phase flow in a square capillary network. In a predominantly experimental work Arriola et al. (1983) investigated the mobilization of oil droplets by surfactants and the resulting droplet snap-off in a constricted square capillary. Finally, Roof (1970) studied the snap-off of nonwetting oil droplets, which is very similar to the snap-off of nonwetting gas bubbles, in a constricted cylindrical capillary with a groove filed into the wall. In this work he developed a static criterion for snap-off that will be described later. However, no one has yet quantified the dynamics of snap-off in noncircular pores. This is our objective.

It is the curvature-driven flow of the wetting liquid along the capillary walls that controls the dynamics of the snap-off of a nonwetting bubble. One substantial difference between snap-off in circular and noncircular pores is the wetting-liquid flow behavior. In cylindrical capillaries the wetting liquid flows along the thin films of liquid that line the pore walls. However, in capillaries of noncircular cross section the wetting flow occurs primarily in the corner regions. Legait (1983) and Singhal and Somerton (1970) have studied two-phase flow problems in square and triangular capillaries, respectively. In addition, the problem of wetting liquid flow along the corners of a predominantly gas-occupied noncircular pore has been solved by Ransohoff and Radke (1986b); it is from this latter paper that the dimensionless flow resistance required to quantify the snap-off process is obtained.

We develop a hydrodynamic model to predict the dynamic breakup of a gas bubble moving through a smoothly constricted noncircular capillary. Calculations are presented for the time to snap-off as a function of the capillary number with the dimensionless resistance to wetting-liquid flow along the corners as a parameter. The calculated snap-off times are compared with experimental data obtained by Gauglitz (1986).

Correspondence concerning this paper should be addressed to C. J. Radke.
T. C. Ransohoff is currently with Kelsius, Inc., San Carlos, CA. P. A. Gauglitz is currently with 3M, St. Paul, MN.

Theory

The snap-off of a gas bubble moving at a constant flow rate through a constricted noncircular capillary is illustrated in Figure 1. As the bubble invades the constriction, the mean curvature of the gas-liquid interface C_m increases so that the bubble front may squeeze into the constriction. After the front has passed the tightest part, or neck, of the constriction, the interfacial curvature begins to decrease. As is explained in the analysis that follows, this drop in curvature, if sufficiently large, initiates a wetting-liquid pressure gradient directed from the front of the bubble to the neck of the constriction. Liquid flows into the constriction, and eventually enough liquid may accumulate at the constriction neck to block the pore and snap off a gas bubble.

As the gas bubble moves through the noncircular capillary, it leaves liquid behind in the corner regions of the capillary, as seen in the cross-sectional view presented in Figure 2. Of course, there will also be wetting liquid left behind in thin films along the straight sections of the capillary. However, the amount of liquid in the films is generally much less than that in the corner regions. Therefore, the thin films are neglected throughout the bulk of our analysis; their effect, which is secondary, is considered at the end of this section.

As will be demonstrated, the wetting-liquid flow along the corners controls the time to snap-off, so as an initial step it is necessary to determine the local amount of liquid deposited in the corners (i.e., the local interfacial curvature) as the bubble front moves through each part of the constriction. Due to the low resistance to liquid rearrangement in the corners compared to

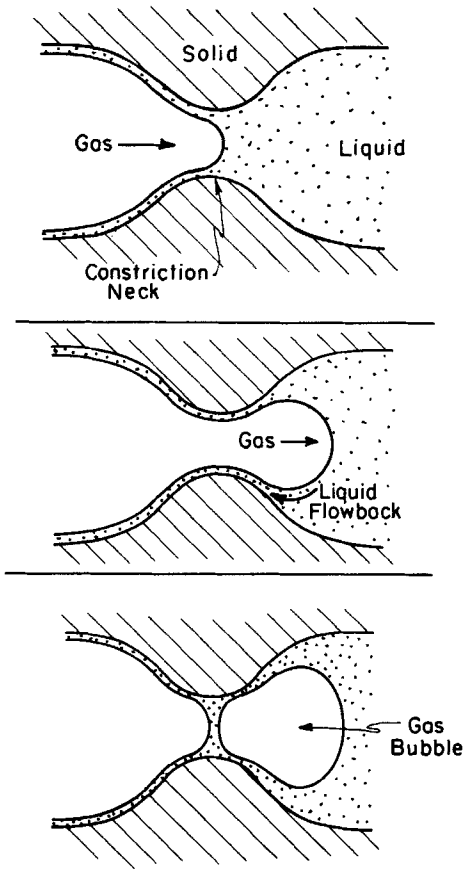

Figure 1. The snap-off process.

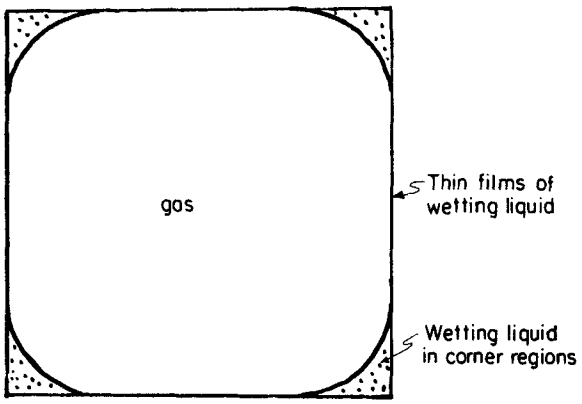

Figure 2. Cross-sectional view: wetting-liquid distribution in a square capillary after a gas bubble has invaded.

that in the thin films, the initial curvature of the interface deposited by the bubble at any axial position equals the curvature of the bubble front passing through that axial position. For smoothly constricted capillaries, we assert that the interfacial curvature at the front of the bubble adjusts immediately to the equilibrium configuration so that, regardless of the bubble velocity, the amount of liquid initially deposited in the corners is set by the equilibrium or minimum surface energy curvature.

The local bubble-front curvature corresponding to the minimum surface energy can be uniquely determined following Mayer and Stowe (1965), as described in the Appendix. Values are presented in Table 1 for the equilibrium dimensionless interfacial curvature, $\tilde{C}_m = C_m R$, in a variety of noncircular cross sections, where R is the local radius of the largest inscribed circle of the capillary. Notice that the interface in a noncircular pore always has a lower curvature than a hemisphere of radius R.

Since the mean curvature of the interface C_m is inversely proportional to the local radius of the capillary, the interfacial curvature of the gas-liquid interface increases as the bubble is

Cross-Sectional Shape	Diagram	$\tilde{C}_m$
Circle		2.00
Square (Legait, 1983)		1.89
Four Beads (Mayer and Stowe, 1965)	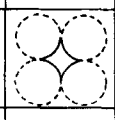	1.86
Equilateral Triangle		1.77
Three Beads (Mayer and Stowe, 1965)	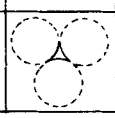	1.75

Table 1. Dimensionless Interfacial Curvatures for Capillaries of Different Cross-sectional Shapes

Thin films are neglected; contact angle Ψ assumed to be 0°.

forced into the constriction. The mean curvature is directly related to the capillary pressure P_c through the Young-Laplace equation,

$$P_c = p_g - p_l = \sigma C_m, \tag{1}$$

where p_g is the pressure in the gas phase, p_l is the pressure in the wetting liquid, and σ is the surface tension. Therefore, as the bubble squeezes into the constriction the capillary pressure rises. Likewise, as the bubble emerges from the neck of the constriction the capillary pressure and interfacial curvature at the bubble front decrease. The difference between the initial interfacial curvatures in the unconstricted section of the tube and in the neck, or throat, of the constriction results in a capillary pressure drop from the throat to the wide section of the capillary. Since it is assumed in this analysis that the gas phase is inviscid, p_g will be constant with respect to axial position, and the capillary pressure drop is equivalent to an axial, wetting-phase pressure gradient for liquid flow from the bubble front in the unconstricted tube section into the neck of the constriction.

The curvature gradients established by the moving bubble front cause the wetting liquid to flow into the pore throat, until the interfacial curvature in the neck approaches that of the bubble front. To determine whether snap-off will occur as the interface nears constant curvature, the stability of the liquid distribution in a noncircular pore must be examined. Qualitative arguments reveal that the gas-liquid interface in the corner of a noncircular pore is stable to small perturbations. The reason for this stability can be seen by considering a small local increase in liquid saturation at the interface, as shown in Figure 3a. The curvature of the saturation disturbance in a corner, C_{m2}, is lower than the average local curvature, C_{m1}. The inviscid gas-phase pressure is constant, so the liquid pressure will be highest in the region of highest liquid saturation, causing liquid to flow out of this region and healing the disturbance. However, when the interfaces from two corner regions meet, as shown in Figure 3b, the curvature at that axial position reaches a minimum value corresponding to the critical capillary pressure for snap-off. Once this critical curvature is attained, a local increase in liquid saturation results in a capillary pressure rise, or a liquid pressure drop. At this point the interface loses its stability, because as liquid flows in from the surroundings it causes an even greater capillary pressure rise. It is assumed that snap-off occurs essentially instantaneously at this point. Growth rates estimated from the linear stability analysis of Goren (1962) support this assumption because at the onset of snap-off, the liquid-filled regions of a noncircular capillary exhibit even less viscous resistance than the thin liquid films in a circular capillary. More important, the experimental observations of Gauglitz (1986) for constricted square pores indicate that collar formation is very rapid compared to the rest of the snap-off process.

Other major differences in the snap-off behavior of nonwetting bubbles in circular and noncircular capillaries can be deduced from the stability arguments presented above. First, as seen later, snap-off in noncircular pores requires a constriction of a certain critical magnitude or greater, whereas it has been shown both theoretically and experimentally (Gauglitz, 1986; Goren, 1962) that snap-off can occur in unconstricted circular capillaries. Second, stable liquid collars are predicted and experimentally confirmed in both constricted and unconstricted circular capillaries when the initial liquid film is very thin (Gauglitz, 1986; Mohanty, 1981). However, in constricted noncircular capillaries such stable collars have not been observed and indeed are not likely due to the large amount of liquid held in the corners.

Since collar formation is rapid, the time to snap-off in a noncircular pore is controlled solely by the wetting-liquid flow along the corners. The corner flow problem, whose geometry is illustrated in Figure 4, has been solved numerically by Ransohoff and Radke (1986b). The solution to this problem is presented in

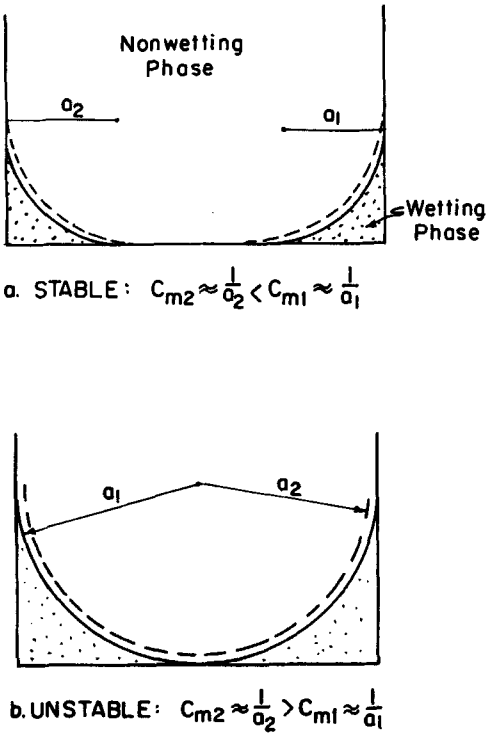

Figure 3. Point of instability or critical curvature in a noncircular capillary.
----- Local saturation disturbance

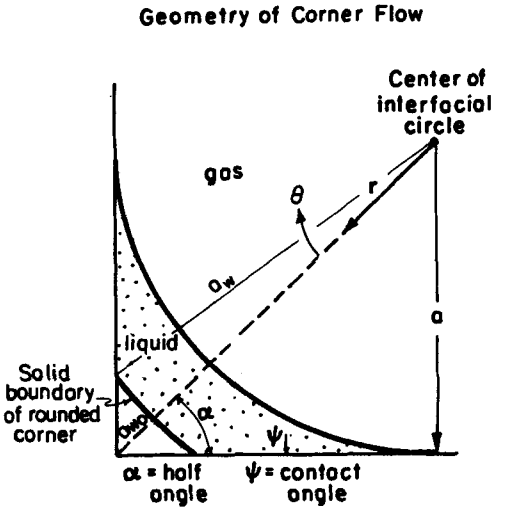

Figure 4. Geometry of the corner-flow problem.

the form of a dimensionless flow resistance β, which is defined:

$$\beta = \frac{a^2}{\mu \langle v_z \rangle} \left(- \frac{dp_l}{dz} \right), \tag{2}$$

where a is the radius of the interfacial circle, μ is the wetting-liquid viscosity, p_l is the wetting-liquid pressure, z is the axial coordinate, and $\langle v_z \rangle$ is the average axial velocity. Values for the dimensionless flow resistance are available (Ransohoff and Radke, 1986b) in terms of the characteristic geometry of the corner flow area [half-angle α, and degree of roundedness $Ro = (a_{wo} - a_w)/(a_{wo} - a)$], the contact angle Ψ, and the dimensionless rigidity of the interface $\mu_s/a\mu$, where μ_s is a Boussinesq, or shear-independent, surface shear viscosity. In reality, the rigidity of the interface could be caused by a number of other phenomena, such as surface tension gradients or surface dilatational dissipation.

Although the time for the wetting-liquid corner flow into the constriction, t_c, is of primary importance to the dynamics of snap-off in constricted noncircular capillaries, a second time scale also arises: the time for the bubble to move through the downstream side of the constriction, t_b. Competition between these two time scales is paramount. If t_b is much greater than t_c, then the bubble moves through the constriction so slowly with respect to the time required for corner liquid readjustment that the liquid in the neck of the constriction is always in equilibrium with the liquid in front of the bubble. Therefore, snap-off occurs as soon as the bubble-front capillary pressure dips below the critical value, and the static breakup criterion presented in the following section applies. Conversely, if t_b is much smaller than t_c, the bubble moves through the constriction so rapidly that when the bubble front reaches the unconstricted section of the capillary, the curvature at the gas-liquid interface is essentially the same as the curvature initially "deposited" by the bubble front. In this case, the dynamics of snap-off are dominated by the wetting-liquid flow along the corners into the capillary neck.

We first address the question of how tight a constriction must be in order for snap-off to occur in a noncircular pore. The answer is presented in the form of a "static" criterion for snap-off in noncircular pores after a similar treatment by Roof (1970). Next, we consider how long it takes for snap-off to occur. A dynamic analysis is presented for determining the time to snap-off based on the two primary time scales discussed above, t_b and t_c, as a function of capillary geometry, fluid properties, and gas-bubble velocity. Finally, the effect of the thin films of wetting liquid on the time to snap-off is pursued. Comparison is made to experimental results in the last section of this paper.

Static criterion for snap-off in a noncircular pore

Roof's analysis (1970) of the snap-off of oil droplets in toroidal constrictions provides the static criterion for snap-off of a perfectly nonwetting phase that has invaded the neck of a constriction. When gravity is neglected, the bubble exhibits a constant-curvature surface. Thus, in Roof's analysis, the wetting-liquid flow required to maintain a constant interfacial curvature is assumed to be so fast that the mean interfacial curvature in the neck of the constriction, C_{mc}, is always equal to that at the bubble front in the unconstricted section of the tube, C_{mT}. By the energy-minimization process described above, C_{mT} is related to the dimensionless interfacial curvature, $\tilde{C}_m$, and the radius of the largest inscribed circle in the straight section of the capillary, R_T, by $C_{mT} = \tilde{C}_m/R_T$. Thus according to Roof's arguments, we have

$$C_{mc} = C_{mT} \equiv \frac{\tilde{C}_m}{R_T}. \tag{3}$$

Again, values of $\tilde{C}_m$ are given in Table 1 for various cross-sectional geometries.

The liquid distribution in a noncircular capillary becomes unstable to snap-off when the interfacial curvature decreases to the critical value C_m^*, corresponding to the curvature of the largest inscribed circle, as shown in Figure 3b. When this distribution is reached, Roof suggests, as we do, that the resulting instability grows so quickly that snap-off occurs essentially instantaneously. The static analysis predicts that snap-off will occur at the neck of the constriction because C_m^* is highest at the throat. Therefore, C_{mc}^* is the critical curvature for snap-off in a noncircular pore; it can be expressed in terms of the two principal radii of curvature as follows,

$$C_{mc}^* = \frac{1}{R_c} - \frac{1}{R_\lambda(0)}, \tag{4}$$

where R_c is the radius of the largest inscribed circle at the constriction neck, and $R_\lambda(0)$ is the transverse interfacial radius of curvature at the neck, which is related to the shape of the constriction.

Therefore, if the curvature of the gas-liquid interface drops below the critical value of C_{mc}^*, then according to the static analysis, snap-off occurs immediately. With Eqs. 3 and 4, the inequality $C_m \le C_{mc}^*$ can be rewritten to give the following expression:

$$\frac{\tilde{C}_m}{R_T} \le \frac{1}{R_c} - \frac{1}{R_\lambda(0)}. \tag{5}$$

Equation 5 can be rearranged as follows to produce a static criterion for snap off,

$$R_T \ge \frac{\tilde{C}_m R_c R_\lambda(0)}{(R_\lambda(0) - R_c)}. \tag{6}$$

The criterion is strictly geometric and states that if the unconstricted tube radius is greater than the right side of Eq. 6, then snap-off will occur; otherwise the bubble will remain intact.

If the transverse radius of curvature $R_\lambda(0)$ is much greater than R_c, then the criterion in Eq. 6 reduces to the following simple expression:

$$R_T \ge \tilde{C}_m R_c. \tag{7}$$

As an example, consider a constriction whose shape is given by the following cosine function, as illustrated in Figure 5,

$$\lambda(\tilde{z}) = 1 - \left(\frac{1 - \lambda_c}{2} \right) [1 + \cos(2\pi\tilde{z})], \tag{8}$$

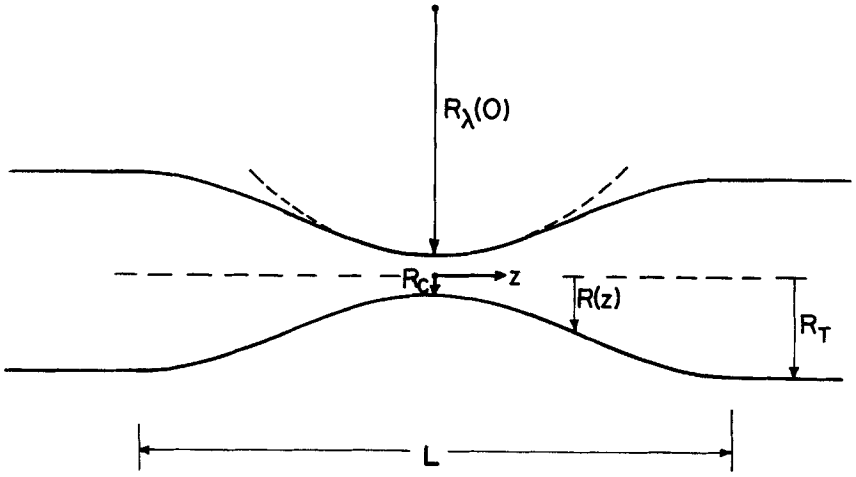

Figure 5. Geometry of the capillary constriction.

where $\lambda(\tilde{z}) = R(\tilde{z})/R_T$, $\lambda_c = R_c/R_T$, and $\tilde{z}$ is the dimensionless axial position, $\tilde{z} = z/L$. z is the axial position measured from the neck of the constriction, and L is the constriction wavelength. The cosine function given in Eq. 8 accurately represents the carefully constricted square capillaries that we use in the snap-off experiments described later. With this shape function, the following expression for the transverse radius of curvature of the interface at the constriction neck, $R_\lambda(0)$, can be calculated, as described in detail elsewhere (Ransohoff, 1986):

$$\frac{R_\lambda(0)}{L} = \frac{L}{R_T}\left[\frac{1}{2\pi^2(1-\lambda_c)\sin\alpha}\right], \tag{9}$$

where α is the half-angle of the corner. Equation 9 reveals that for a constriction with L/R_T equal to about 10, $R_\lambda(0)$ is approximately equal to L; for larger values of L/R_T, $R_\lambda(0)$ is greater than L. In these cases, $R_\lambda(0)$ is much greater than R_c and may be safely neglected in calculation of the curvature.

The analysis presented in this paper uses the assumption that the capillary is smoothly constricted (i.e., that $L/R_T > 10$), and therefore the contribution to the interfacial curvature due to the axial shape of the constriction is neglected. The applications of our problem generally lie in porous media that certainly exhibit some sharply constricted pores. However, snap-off is actually less likely in sharply constricted geometries because a smaller transverse radius of curvature (i.e., a smaller $R_\lambda(0)$ in Eq. 4) decreases the mean curvature of the constriction. That is, a large axial curvature, i.e., a sharp constriction, stabilizes the liquid-gas interface against snap-off. Indeed, Legait (1983) constructed sharp corners in a constricted square capillary and did not observe snap-off. Therefore, the assumption of a smooth constriction is both convenient and relevant to foam generation in porous media.

The static criterion of Eq. 7 is very useful in predicting whether snap-off will occur in a constriction of noncircular cross section. However, it provides no information concerning the time required for snap-off or the size of the bubbles generated. To predict the time to snap-off, the dynamics of the snap-off process must be described.

Time required for a bubble to move through a constriction

The differential time interval dt required for a bubble moving at velocity $u_g(z)$ to pass through a differential axial length of the capillary dz is given by definition as

$$dt = \frac{dz}{u_g(z)}. \tag{10}$$

For the case of an incompressible bubble moving at constant flow rate through a constriction of constant cross-sectional shape, $u_g(z)$ can be calculated from the bubble velocity in the unconstricted section, u_T,

$$u_g(z) = \frac{u_T R_T^2}{R(z)^2}. \tag{11}$$

Let the length element z in Eq. 10 be scaled by the wavelength of the constriction, L, and the local radius $R(z)$ be scaled by R_T, the radius of the largest inscribed circle in the unconstricted section of the capillary. Equations 10 and 11 then combine to read

$$d\tilde{t} = \lambda(\tilde{z})^2 d\tilde{z}, \tag{12}$$

where $\lambda(\tilde{z}) = R(\tilde{z})/R_T$, $\tilde{z} = z/L$, and $\tilde{t} = tu_T/L$.

To calculate t_b, the time required for a bubble to move through the downstream side of a constriction of length L, Eq. 12 is integrated:

$$\int_0^{\tilde{t}_b} d\tilde{t} = \tilde{t}_b = \int_0^{1/2} \lambda(\tilde{z})^2 \, d\tilde{z}. \tag{13}$$

When the shape of the constriction is modeled by the cosine function given in Eq. 8, Eq. 13 yields

$$\tilde{t}_b = \frac{3}{16} + \frac{\lambda_c}{8} + \frac{3\lambda_c^2}{16}. \tag{14}$$

As expected, bubbles move slightly faster through the downstream side of a tighter constriction than of a looser one; a plot of $\tilde{t}_b$ as a function of λ_c is given in Figure 6. The indicated limiting

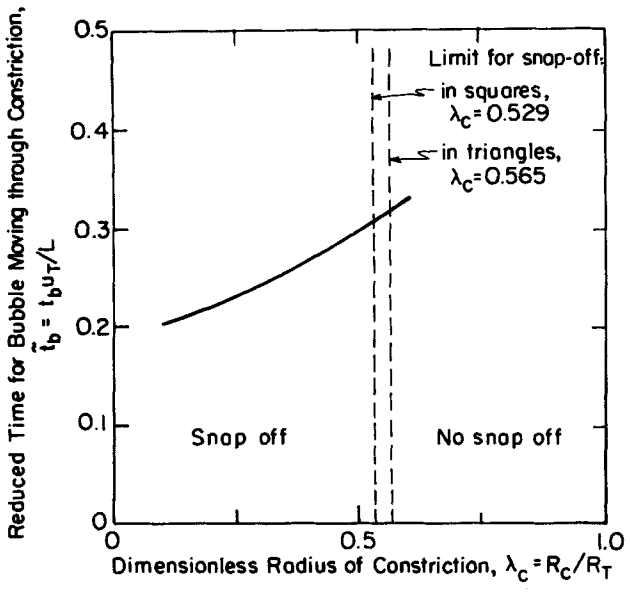

Figure 6. Dimensionless time for a bubble to move through a constriction $\tilde{t}_b$ as a function of λ_c.

---- Transition between capillary geometries that allow snap-off and those that do not.

values of λ_c for snap-off in equilateral triangular and square capillaries are based on the static snap-off criterion of Eq. 7.

Equation 14 provides an upper bound on t_b for two reasons. First, the assumption of an incompressible bubble used in this analysis is questionable for gas bubbles passing through tight constrictions at low velocities (Gauglitz, 1986); a compressible bubble will move through the downstream half of the constriction more quickly than an incompressible bubble. Second, t_b should not be the time required for the bubble to move through the entire constriction; rather, it should be the time for the bubble to move from the neck of the constriction to the axial position $\tilde{z}^*$ at which the static snap-off criterion is first met. The bubble will nearly always reach the critical axial position $\tilde{z}^*$ before it reaches the end of the constriction.

It is important to note that the effects of the nonwetting bubble velocity and constriction length on the time for the bubble to flow through the constriction, $t_b = \tilde{t}_b L/u_T$, are both contained in the characteristic time L/u_T. Therefore, t_b can be calculated given the shape function of the constriction $\lambda(\tilde{z})$, the length of the constriction L, and the nonwetting bubble velocity in the unconstricted section of the capillary u_T. In the next section we address the calculation of other major characteristic time in this problem, t_c, the time to snap-off due to "flowback" of the wetting liquid.

An evolution equation for corner flow time

Calculation of t_c requires the solution to the problem of the flow of a wetting liquid from the front of a gas bubble into the throat of the constriction of a noncircular capillary to cause snap-off. The thin films of wetting liquid, which are important in the dynamics of snap-off in a circular pore, are neglected in this analysis. Their secondary effect is considered later.

To begin the analysis, the relationship between flow along the corners and accumulation of liquid in the constriction, which will eventually lead to snap-off, is described by a continuity equation for the liquid phase:

$$\frac{\partial A_l}{\partial t} = -\frac{\partial q_l}{\partial z}, \tag{15}$$

where A_l is the cross-sectional area available for wetting-liquid flow along the corners, and q_l is the wetting-liquid volumetric flow rate. Upon neglect of viscous dissipation in the gas phase, q_l is related by Eq. 2 to the local liquid pressure drop, dp_l/dz, through the dimensionless flow resistance for flow along a corner β, as described by Ransohoff and Radke (1986b),

$$q_l = \frac{a^2(z) A_l}{\mu\beta}\left(-\frac{dp_l}{dz}\right), \tag{16}$$

where μ is the wetting-fluid viscosity.

As discussed previously, the assumption of a smoothly constricted capillary permits neglect of the transverse curvature, making the circumferential radius of curvature $a(z)$ the only important curvature component, so that $C_m(z) = 1/a(z)$. The Young-Laplace expression is then differentiated with respect to z to establish the liquid-phase pressure gradient,

$$\frac{dp_l}{dz} = -\frac{d}{dz}\left[\frac{\sigma}{a(z)}\right] = \frac{\sigma}{a^2(z)}\frac{da}{dz}. \tag{17}$$

Combining Eqs. 15–17 and using the fact that A_l is proportional to a^2 yields an evolution equation, which describes the interfacial radius of curvature as a function of position and time,

$$\frac{\partial \kappa}{\partial \tilde{t}} = \kappa\frac{\partial^2 \kappa}{\partial \tilde{z}} + 2\left(\frac{\partial \kappa}{\partial \tilde{z}}\right)^2, \tag{18}$$

where $\kappa = a/R_T$ is the dimensionless interfacial radius of curvature, $\tilde{z} = z/L$, and $\tilde{t} = t/\tau_c$. τ_c is the characteristic time for liquid flow and is equal to $[2\mu\beta R_T(L/R_T)^2]/\sigma$. In Eq. 18 the assumption is made that the dimensionless flow resistance β is a constant, independent of position or time. This assumption is correct for flow of a fluid exhibiting a no-stress or a no-slip interface in a capillary with sharp corners and constant cross-sectional shape. When there is a finite surface shear viscosity (i.e., neither a no-stress nor a no-slip interface), or the corners are rounded, or the cross-sectional shape changes with axial position, then the assumption is not correct. However, if β is taken as a function of axial position, time, or both, the solution to the problem becomes much more difficult. In this study, the dimensionless flow resistance is always assumed to be a constant; in the cases where this assumption is not strictly valid, we use an average value of β based on the appropriate limiting values of surface shear viscosity, corner roundedness, or cross-sectional shape.

Equation 18 is solved numerically using a Galerkin finite-element technique with a Crank-Nicolson time-stepping scheme to give κ as a function of position and time in a constriction with a shape function given by Eq. 8. A detailed description of the numerical techniques is given elsewhere (Ransohoff, 1986). As shown in Figure 3, snap-off occurs when $C_m(z) = 1/[R(z)]$, or in dimensionless form, when $\kappa(\tilde{z}) = \lambda(\tilde{z})$. As expected, the solution to Eq. 18 demands that snap-off commence at $\tilde{z} = 0$, the neck of the constriction, for large values of λ_c. However, as λ_c

approaches zero the snap-off position moves slightly downstream from the neck of the constriction to a dimensionless axial position of around $\tilde{z} = 0.05$. One implication of this result is that the amount of liquid flow required for snap-off in an infinitely tight constriction is finite. Therefore, as λ_c approaches zero the dimensionless time for corner flow t_c approaches a nonzero value that is slightly dependent on the geometry of the constriction. The nonzero asymptote can be seen in Figure 7, which is a plot of the reduced time to snap-off by corner flow, $\tilde{t}_c$, as a function of the dimensionless constriction radius λ_c for capillaries of both square and equilateral triangle cross sections. It is evident that there is little effect of λ_c on $\tilde{t}_c$ for tight constrictions. However, as λ_c approaches $1/\tilde{C}_m$, which is the maximum value at which snap-off is still possible, the driving force for liquid flow becomes infinitesimal and the corresponding snap-off time increases dramatically.

The effects of fluid properties, constriction length, corner geometry, and pore size on the time for liquid flow to cause snap off, $t_c = \tilde{t}_c \tau_c$, are embodied in the characteristic time for liquid flow, $\tau_c = [2\mu R_T \beta (L/R_T)^2]/\sigma$. From the form of τ_c, it is clear that the time for liquid flow is directly proportional to the square of the normalized constriction length L/R_T, directly proportional to the viscosity of the liquid μ, and inversely proportional to σ/R_T, which represents the tension driving force for liquid flow. The effects of surface shear viscosity, corner geometry, and contact angle are contained in the dimensionless flow resistance β, which is calculated as a function of these variables elsewhere (Ransohoff and Radke, 1986b).

Calculation of time to snap-off in noncircular pores

The overall time to snap-off of a gas bubble in a constricted noncircular capillary can now be determined. The calculation is started at $t = 0$, which is set to the time when the bubble front reaches the neck of the constriction. Values for the dimensionless time for a bubble to move through the constriction, $\tilde{t}_b$, and for the dimensionless time for liquid to flow back into the tight part of the constriction, $\tilde{t}_c$, are obtained from Figures 6 and 7 for the specified capillary geometry. These dimensionless times can be multiplied by their respective characteristic times to establish t_b and t_c. The maximum of t_b and t_c is then taken to be the time to snap-off, t_{so}, which is reduced by the characteristic time $\tau_{so} = \mu R_T/\sigma$. In this section $\tilde{t}_{so} = t_{so}/\tau_{so}$ is calculated as a function of the capillary number; the resulting theory is later tested against the experimental data of Gauglitz (1986).

An example calculation of t_{so} is presented here for a constricted square pore with $\lambda_c = 0.3$ and $L/R_T = 20$. $\tilde{t}_b$ is determined for the given conditions from Figure 6 to be approximately equal to 0.24. The actual time required for the bubble to move through the constriction, t_b, can then be calculated as

$$t_b = \frac{\tilde{t}_b L}{u_T} = \frac{4.8 R_T}{u_T}. \tag{19}$$

Likewise, $\tilde{t}_c$ is determined from Figure 7 for the given constriction shape to be 0.073, permitting t_c to be calculated:

$$t_c = \tilde{t}_c \tau_c = \frac{58 \beta \mu R_T}{\sigma}. \tag{20}$$

As described above, the dimensionless time to snap-off, $\tilde{t}_{so}$, is written as follows,

$$\tilde{t}_{so} = \frac{\max |t_b, t_c| \sigma}{\mu R_T}. \tag{21}$$

Values of $\tilde{t}_{so}$ are obtained as a function of the capillary number, $Ca = \mu u_T/\sigma$, with β as a parameter; results are plotted in Figure 8. Notice that the contribution to the time to snap-off due to t_c is

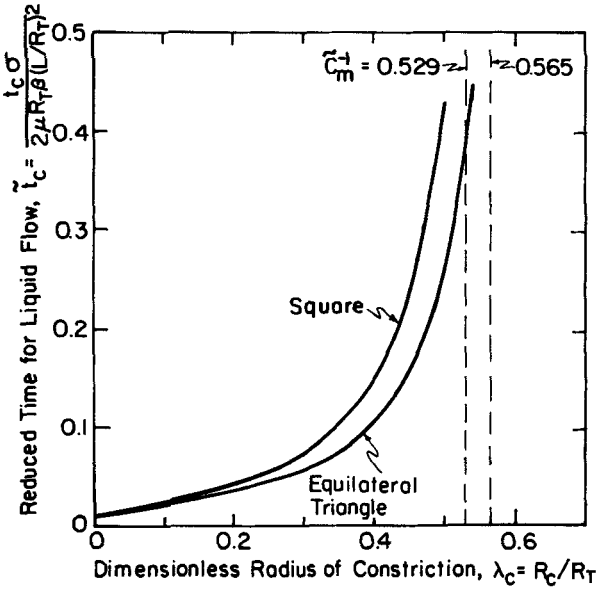

Figure 7. Dimensionless time for liquid flow into a constriction to cause snap-off $\tilde{t}_c$ as a function of λ_c.

---- Transition between capillary geometries that allow snap-off and those that do not.
Calculations are for capillaries of square and equilateral triangle cross sections.

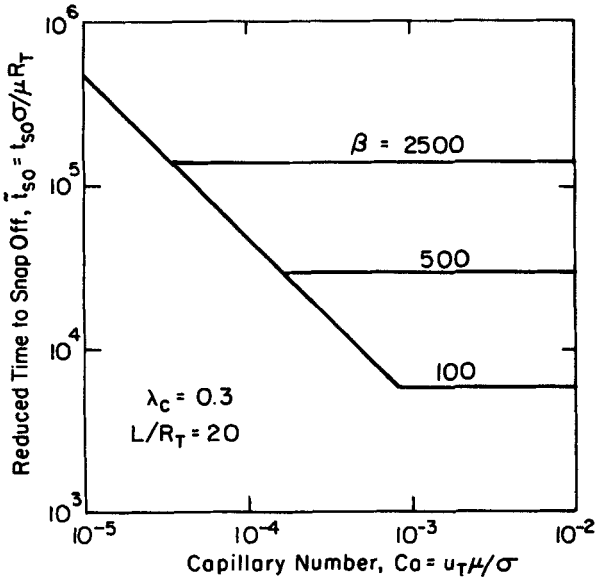

Figure 8. Dimensionless time to snap-off $\tilde{t}$, as a function of the capillary number *Ca*, over a range of values for dimensionless corner flow resistance β.

The capillary considered is square with $\lambda_c = 0.3$, $L/R_T = 20$.

independent of the capillary number, while the contribution from t_b is inversely proportional to Ca. There is a transition capillary number at which the time to snap-off changes from the time for the bubble to move through the constriction, t_b, to the time for the liquid flow causing snap-off, t_c. It is evident that the dimensionless flow resistance β strongly affects the contribution of t_c. As β increases, the transition capillary number decreases and t_c becomes a more important contribution to the snap-off time.

The effect of λ_c on the time to snap-off is considered by performing the same calculation for $\lambda_c = 0.4$ and $L/R_T = 20$, the results of which are plotted in Figure 9. Comparison of Figures 8 and 9 shows that increasing λ_c does not significantly change the value of t_b, but it does significantly increase the contribution of t_c. This result is expected in light of the dependencies of t_b and t_c on λ_c, displayed in Figures 6 and 7, respectively.

So far, the thin films of wetting liquid that line the straight sections of the noncircular capillary have been neglected in the dynamic snap-off analysis. In the next section, the effect of thin films on the time to snap-off is considered.

Effect of thin films

When a bubble front moves through a noncircular capillary, thin films of wetting liquid are deposited along the straight sections in addition to the liquid left behind in the corner regions. A cross-sectional view of the initial distribution of wetting liquid is illustrated in Figure 10a. An analysis of the initial film thickness laid down by a bubble moving through a circular capillary was first performed by Bretherton (1961). This analysis has not been extended to noncircular capillaries. However, based on Bretherton's theory, we expect the initial dimensionless film thickness in a noncircular pore, $\tilde{h}_o = h_o(z)/R(z)$, to be proportional to the capillary number raised to some power. Compared to the case where the thin films are neglected, the presence of thin films

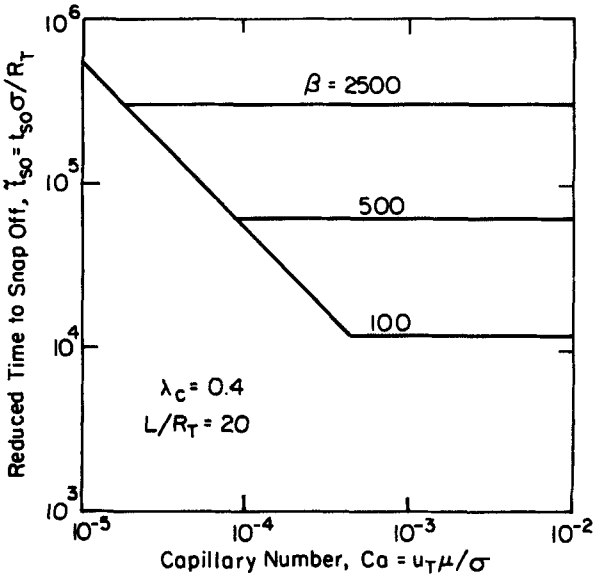

Figure 9. Dimensionless time to snap off $\tilde{t}_{so}$ as a function of the capillary number *Ca* over a range of values for dimensionless corner flow resistance β.

The capillary considered is square with $\lambda_c = 0.4$, $L/R_T = 20$.

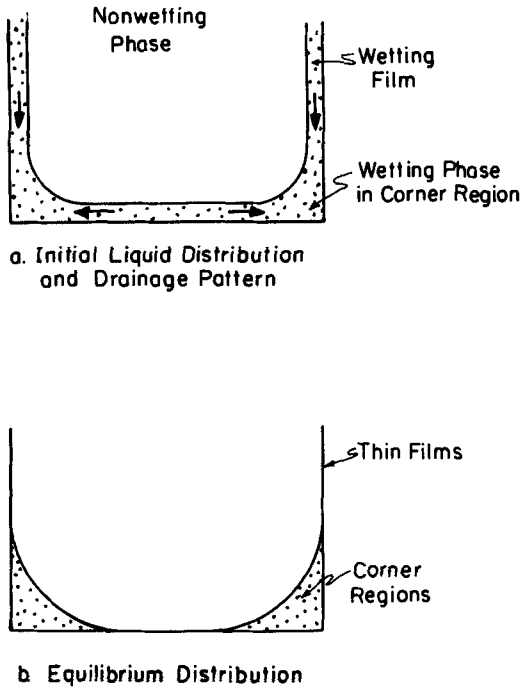

Figure 10. Initial and equilibrium distributions of liquid, considering the thin films of wetting liquid deposited along the straight sections of the pore in a noncircular capillary.

increases the wetting liquid saturation, S_l, at any axial position. The saturation in the presence of thin films can be determined by simple geometrical arguments; for example, the saturation in a square pore is

$$S_l = \frac{(4-\pi)}{\tilde{A}\tilde{C}_m^2} + \left(8 - \frac{8-2\pi}{\tilde{C}_m^2}\right)\frac{\tilde{h}_o}{\tilde{A}} - \left(2 - \frac{4-\pi}{\tilde{C}_m^2}\right)\frac{\tilde{h}_o^2}{\tilde{A}^2}, \quad (22)$$

where $\tilde{C}_m$ is the previously defined dimensionless interfacial curvature, and $\tilde{A}$ is the capillary cross-sectional area divided by $R(z)^2$.

As time progresses, the liquid in the thin films drains into the corner regions due to a capillary pressure gradient between the flat thin films and the curved corner regions. This drainage process, which is depicted in Figure 10a, is similar to the drainage of liquid in foam and emulsion lamellae into the Plateau borders (Adamson, 1976). Eventually, an equilibrium film thickness may be attained where the magnitude of the disjoining pressure in the thin films equals the magnitude of the capillary pressure in the corner regions (Clunie et al., 1971). An evolution equation, from which the time for film drainage t_f can be calculated, is derived elsewhere (Ransohoff, 1986) The characteristic time of the drainage process arises naturally from the scaling of this evolution equation and has the form $\tau_f = [\mu\beta_f R(z)]/\sigma\tilde{h}_o^3$, where β_f is the dimensionless flow resistance for flow along the film.

If t_f is much greater than the time to snap-off, the thin films will not drain into the corner regions before snap-off occurs. Therefore, the distribution of liquid in the capillary will remain as illustrated in Figure 10a, and the effect of the thin films will be to reduce the local characteristic dimension of the pore, $R(z)$. By decreasing the effective size of the pore, the thin films

increase the critical capillary pressure required for snap-off in the neck of the constriction, meaning that snap-off can occur more quickly. In addition, for a given interfacial radius of curvature, the area available for liquid flow at any axial position will be larger. Therefore β, the dimensionless flow resistance for flow along the corners, will diminish. Finally, the bubble will almost certainly be moving faster near the throat of the constriction than in the unconstricted section of the tube, which, according to Bretherton's analysis (1961), causes h_o to be greater near the constriction neck. The effect of a relatively thicker film in the neck of the constriction is to increase the driving force for flow into the constriction over its value for the case in which the thin films are neglected. These factors all contribute to a decrease in the time to snap-off as the film thickness increases.

If t_f is much smaller than the snap-off time, then the liquid deposited in the capillary will rearrange quickly into the configuration shown in Figure 10b. In this case the relationship between the initially deposited saturation, S_l, which is determined from Eq. 22, and the resulting dimensionless interfacial curvature, $\tilde{C}_m$, is written in Eq. 23 for the case of a square capillary.

$$\tilde{C}_m = \frac{1}{2}\left(\frac{4-\pi}{S_l}\right)^{1/2} \tag{23}$$

The effect of drainage of the thin films is to decrease the resulting curvature of the interface by increasing the liquid saturation at all points along the capillary. This will cause the dimensionless flow resistance β to decrease, and will produce an initial configuration at the constriction throat that is closer to the critical snap-off configuration. Again, this leads to quicker snap-off times.

Unlike snap-off in circular pores, where the thin films dominate the physics of the problem (Gauglitz, 1986), the thin films represent only a secondary effect in the problem of snap-off in a noncircular pore. We have shown in this section that the secondary effect of thin films will be to decrease the time to snap-off. Bubbles moving at higher gas velocities lay down thicker films, so a slight decrease in the time to snap-off is expected at higher gas velocities.

Comparison with Experiment

In the experiments performed by Gauglitz (1986), gas bubbles were injected into constricted square pores at constant volumetric flow rates; 16 mm motion pictures recorded the subsequent snap-off events. The time to snap-off was determined by counting the number of frames on the film from the time the bubble reached the neck of the constriction to the time snap-off occurred.

The experiments were carried out for four different wetting liquids. Deionized distilled water (σ = 72 mN/m, μ = 1.0 mPa · s) and a glycerol-water solution (σ = 68 mN/m, μ = 8.5 mPa · s) were used to investigate the effect of wetting-liquid viscosity. To determine the effect of surface active agents, snap-off behavior was also studied in aqueous solutions of sodium dodecyl benzene sulfonate (Sharpe Chem. Co., Burbank, CA, 1 wt. %, σ = 31 mN/m, μ = 1.0 mPa · s) and Chaser SD1000 (Chevron Chem. Co., Richmond, CA, 1 wt. %, σ = 39 mN/m, μ = 1.1 mPa · s), an industrial sodium alkyl disulfonate (Straus et al., 1976). Interestingly, consistent data were difficult to obtain for the water experiments because the disjoining forces resisting the thin-film drainage are so weak that dry patches sometimes formed on the straight sections of the square capillary. For the glycerol-water solution, data reproducibility is within ±10%. With water and surfactant solutions, errors of at most a factor of 2 are seen.

Two constricted square glass capillaries (Wilmad Glass Co., Inc., Buena, NJ) with R_T = 0.5 mm were used in the experiments. Before each experiment, the capillaries were carefully cleaned with chromic acid and thoroughly flushed with deionized distilled water. The "narrow" pore had a dimensionless constriction radius λ_c of about 0.3, and a dimensionless constriction length L/R_T of 16; the "wide" pore had a λ_c of approximately 0.5 and a dimensionless length of 14. Given λ_c and L/R_T, the shape of the constrictions was well approximated by the cosine function in Eq. 8. Unfortunately, it is more difficult to characterize the cross-sectional geometry of the square pores than the constriction geometry. The parameter that is crucial to this particular calculation is the degree of roundedness, *Ro*, which can significantly affect the dimensionless flow resistance β (Ransohoff and Radke, 1986b). When one considers the distribution of liquid in the corners as shown in Figure 11, it is clear that a small filling-in of the corners can have a large effect on the resistance to liquid flow, and it is very difficult to constrict a square capillary without some rounding of the corners. From characterization of the cross sections of the two square pores at

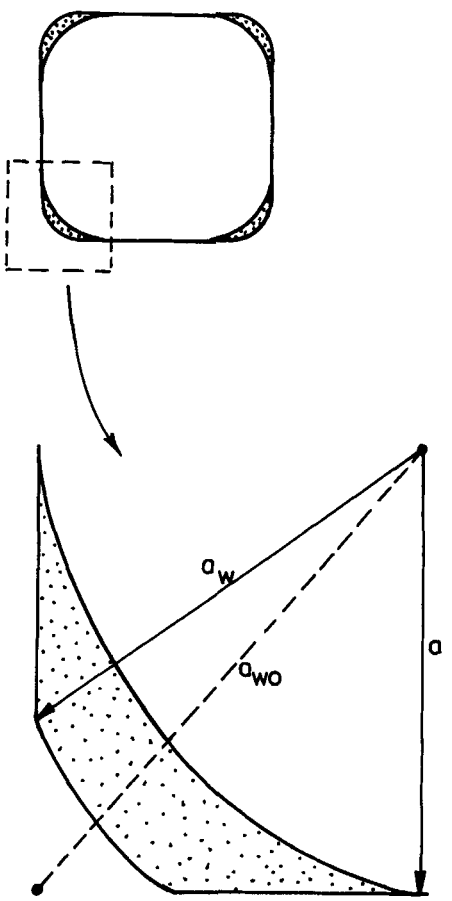

Figure 11. Effect of rounded corners on resistance to flow along the corners of a noncircular pore.

the neck of the constrictions (Gauglitz, 1986), we estimate that on the average the corners are filled in to the extent of approximately 5% of the area of the cross section. This means that throughout the wetting-liquid flowback process, the average value of the degree of roundedness of the corner region, Ro, which is needed for calculating the dimensionless flow resistance, is approximately equal to 0.75.

For a perfectly wetting liquid, $\Psi = 0$, with a no-stress, gas-liquid interface, in a square pore, $\alpha = (\pi/4)$, with a degree of roundedness of $Ro = 0.75$, the dimensionless flow resistance β is calculated to be 760 (Ransohoff and Radke, 1986b) The time to snap-off is then determined as a function of the capillary number by the methods outlined in the previous sections. This theoretical curve is plotted in Figure 12 and is compared to the data for water and the glycerol-water solution (open triangles and circles, respectively) in the narrow pore ($\lambda_c \approx 0.3$).

The theory developed in this paper does a reasonably good job of predicting the time to snap-off, especially since no adjustable parameters are employed. However, two items should be discussed. First, as mentioned previously, the analysis provides an upper limit on t_b due to the compressible nature of the gas bubble and to the fact that the static snap-off criterion is generally met before the bubble front reaches the end of the constriction. Therefore, the theoretical curve for t_b should be shifted to the left, which suggests that it is the theory, not the circled datum at the lowest capillary number, that is incorrect. The second point is that the effect of the thin films, which was discussed in the previous section, can be seen in Figure 12. As predicted, a thicker film is deposited at the higher capillary numbers, causing the time to snap-off to decline.

The experimental results obtained in the narrow pore with the two surfactant solutions (closed triangles and squares) are also presented against the theory in Figure 12. The difference between these results and those for solutions without surfactant can only result from a change in the dimensionless flow resistance. Generally, surfactants make the interface more rigid, either through surface shear viscosity or tension gradients. This rigidity causes an increase in the dimensionless resistance to flow in the corners, β, and therefore in the time for liquid flow, t_c. Given the corner flow parameters introduced earlier for the square pores, $\alpha = (\pi/4)$, $Ro = 0.75$, and $\Psi = 0$, a rigid interface causes β to increase from 760 to 2,800 (Ransohoff and Radke, 1986b). It is evident from Figure 12 that the increase in the time to snap-off due to the presence of surfactants is modeled very well *a priori* by accounting for the rigidity of the interface.

Finally, Figure 13 compares the surfactant-free data for the narrow ($\lambda_c \approx 0.3$) and wide ($\lambda_c \approx 0.5$) pores. These data indicate, as predicted in the theory section, that the time to snap-off increases significantly as the dimensionless radius of curvature λ_c approaches the limiting value for snap-off in a square pore, $\lambda_c^* = 0.529$. However, the time to snap-off in the wide pore appears to be inversely proportional to the capillary number, whereas theory predicts that it should be independent of the capillary number. Although the inverse-capillary number dependence suggests that t_{so} may be equal to t_b over the range of flow rates studied, this explanation is rejected because t_b truly provides an upper limit, and the motion pictures show that the bubble front is very far downstream from the constriction when

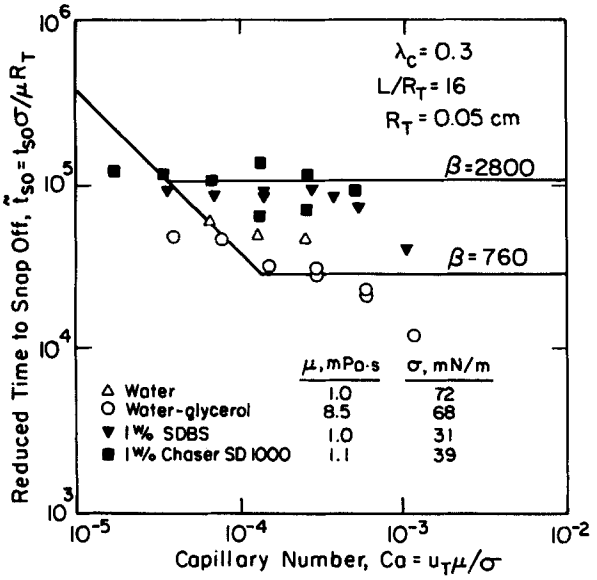

Figure 12. Dimensionless time to snap-off as a function of capillary number.

Data from Gauglitz (1986) for snap-off of gas bubbles in narrow constricted square pore with measured parameters $\lambda_c = 0.3$, $L/R_T = 16$, $R_T = 0.05$.

Δ O Water ($\mu = 1.0$ mPa · s, $\sigma = 72$ mN/m) and water-glycerol solution ($\mu = 8.5$ mPa · s, $\sigma = 68$ mN/m)

▼ ■ 1 wt. % SDBS solution ($\mu = 1.0$ mPa · s, $\sigma = 31$ mN/m) and 1 wt. % Chevron Chaser SD1000 solution ($\mu = 1.1$ mPa · s, $\sigma = 39$ mN/m)

— Predictions from theory with input parameters (λ_c and L/R_T) equal to measured parameters.

β is calculated for a perfectly wetting fluid in a square pore with $Ro = 0.75$, and is equal to 760 for the case of a free interface ($\mu_s = 0$) and 2,800 for a rigid interface ($\mu_s = \infty$).

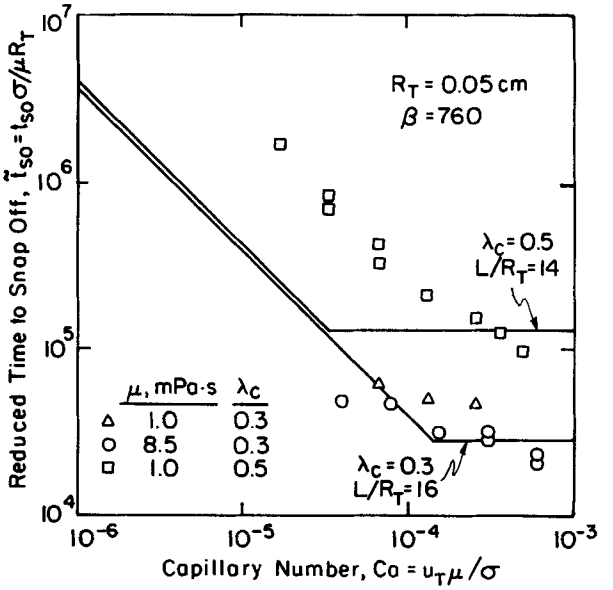

Figure 13. Dimensionless time to snap-off as a function of capillary number.

Data are from Gauglitz (1986) for snap-off of gas bubbles in two constricted square pores of radii $R_T = 0.05$ cm and measured parameters $\lambda_c = 0.3$, $L/R_T = 16$ (narrow pore) and $\lambda_c = 0.5$, $L/R_T = 14$ (wide pore).

Fluids used: water ($\mu = 1.0$ mPa · s, $\sigma = 72$ mN/m) and water-glycerol solution ($\mu = 8.5$ mPa · s, $\sigma = 68$ mN/m)

— predictions from theory with input parameters (λ_c and L/R_T) equal to measured parameters.

β is calculated to be 760 for a perfectly wetting fluid in a square pore with $\mu_s = 0$ and $Ro = 0.75$.

snap-off occurs. It is possible, however, that as λ_c approaches the limiting value for snap-off, the time to snap-off is more sensitive to the initial curvature distribution and therefore is more sensitive to the thickness of the neglected thin films, which is a strong function of the capillary number.

Conclusions

A corner flow hydrodynamic theory is presented for calculating the time to snap-off of a gas bubble moving at constant flow rate through smoothly constricted noncircular capillaries. The time scales that are the most important in this problem are the time for a bubble to move through the downstream side of a constriction, t_b, and the time for liquid to flow back into the constriction neck to cause snap-off, t_c. Assuming an incompressible bubble, an expression is developed for t_b that represents an upper limit on this contribution to the snap-off time. t_c is calculated from a dynamic evolution equation. The maximum of these two times is taken to be the time to snap-off, which is quantified as a function of the capillary number, $Ca = u_T\mu/\sigma$, the dimensionless flow resistance, β, and the shape of the constriction, $\lambda(\tilde{z})$.

We show that above a critical or transition capillary number, the time to snap-off of a gas bubble in a noncircular pore is constant, while below this capillary number the time to snap-off is predicted to be inversely proportional to the capillary number. In addition, the contribution of t_c to the snap-off time is found to increase with increasing values of β and increasing dimensionless constriction radii, λ_c. Finally, the influence of thin films of wetting liquid on the time to snap-off is shown to be secondary; at higher capillary numbers, thicker films are deposited, causing a slight decrease in the time to snap-off.

Theory is compared to experiments conducted in two constricted square capillaries, a narrow capillary with shape parameters $\lambda_c = 0.3$ and $L/R_T = 16$, and a wide capillary with shape parameters $\lambda_c = 0.5$ and $L/R_T = 14$. When the degree of roundedness of the corners is taken into account, the theory does an excellent job of matching the data in the narrow pore with no adjustable constants. Results in the wide pore are in qualitative agreement with the theory in that the time to snap-off becomes much larger as λ_c approaches the limiting value for snap-off. In the narrow-pore experiments, the viscosity of the fluid is varied by nearly an order of magnitude with no significant change in the dimensionless time to snap-off, indicating that the problem is properly scaled. The presence of surfactants augments the time to snap-off; the amount of this increase can be predicted *a priori* by accounting for the interfacial rigidity.

Acknowledgment

This work was supported by United States Department of Energy, Grant No. DE-AC03-76SF00098 to Lawrence Berkeley Laboratories at the University of California. T. C. Ransohoff acknowledges fellowships from the Shell Foundation and the Regents of the University of California. P. A. Gauglitz received financial support from the Shell Development Company.

Notation

a = radius of interfacial circle, m
a_1 = length from corner vertex to interface along pore wall, m
a_w = distance from center of interfacial circle to filled-in corner, m
a_{wo} = distance from center of interfacial circle to sharp corner vertex, m
A = cross-sectional area of capillary, m^2
Ca = capillary number, $u_T\mu/\sigma$, ratio of viscous forces to tension forces
C_m = mean curvature of interface, m^{-1}
C_{mc} = mean curvature of interface at neck of constriction, m^{-1}
$g(\Psi) = \pi - 3\Psi - 6\cos\Psi\sin(\pi/3 - \Psi)$, function used in energy-minimization calculation
h = thin film thickness, m
L = length of constriction, m
$L_{nw,s}$ = perimeter of gas-solid contact in noncircular capillary, m
$L_{nw,w}$ = wetted perimeter in given cross section of noncircular capillary, m
$L' = L_{nw,w} - L_{nw,s}\cos\Psi$, used in energy-minimization calculation, m
p = pressure, $kg/m \cdot s^2$
P_c = capillary pressure, $kg/m \cdot s^2$
q = volumetric flow rate, m^3/s
R = radius of largest inscribed circle in a noncircular cross section, m
R_c = radius of largest inscribed circle at neck of constriction, m
R_λ = transverse interfacial radius of curvature, m
Ro = degree of roundedness of corner
S = saturation or volume fraction of a phase
t = time, s
t_b = time for a bubble to move through downstream side of a constriction, s
t_c = time for liquid flow into constriction that causes snap-off, s
u = superficial velocity, m/s
v_z = wetting-liquid axial velocity, m/s
z = axial position, m

Greek letters

α = half-angle of corner
β = dimensionless flow resistance along a corner
κ = dimensionless interfacial radius of curvature
λ = dimensionless local pore radius
λ_c = dimensionless radius at neck of constriction
μ = viscosity of wetting phase, $kg/m \cdot s$
μ_s = surface shear viscosity, kg/s
σ = surface tension, kg/s^2
τ = characteristic time, s
τ_c = characteristic time for corner flow, s
Ψ = contact angle
ω = angle describing sector of interfacial circle that comprises the interface

Subscripts

f = thin film
g = gas phase
l = liquid phase
o = initial
so = snap-off
T = unconstricted section of the tube
1 = initial
2 = final

Superscripts

$\sim$ = dimensionless
$*$ = critical

Appendix

When a gas bubble front moves through a section of a cylindrical capillary, the radius of curvature of the bubble front is equal to half the radius of the capillary, $R/2$, minus half the thickness of the thin wetting film, $h/2$. Assuming $h \ll R$, the curvature of the deposited interface is set by the pore wall. However, in a noncircular capillary the curvature of the gas-liquid interface is not constrained by the pore walls; it can adjust significantly by moving the interface farther in or out of the corner. Therefore, when a gas-bubble front moves through a noncircu-

lar capillary this extra degree of freedom allows the interfacial curvature to adjust to a minimum surface energy configuration.

The procedure for calculating the minimum energy configuration of a nonwetting bubble front in a noncircular capillary is described by Mayer and Stowe (1965), who begin the analysis by deriving the following expression for the capillary pressure in a noncircular pore throat:

$$P_c = \sigma\left(\frac{L_{nw,w} - L_{nw,s}\cos\Psi}{A}\right) \equiv \sigma\frac{L'}{A}, \qquad \text{(A1)}$$

where $L_{nw,w}$ is the cross-sectional perimeter of the curved gas-liquid interface, $L_{nw,s}$ is the perimeter of the gas-solid interface, Ψ is the equilibrium contact angle, and A is the cross-sectional area occupied by the nonwetting phase. The minimum surface energy configuration is found by minimizing the capillary pressure or, equivalently, by minimizing L'/A. Therefore, for a given contact angle and cross-sectional shape the problem reduces to a complicated exercise in geometry.

Mayer and Stowe calculated the equilibrium configuration in the pore channels resulting from a variety of arrangements of monodisperse beads, and Legait (1983) has performed this calculation for the case of a square capillary. In this appendix a solution for the minimum surface energy configuration in an equilateral triangular capillary is presented to illustrate the calculation. The results of all of these calculations are summarized in Table 1 in terms of a dimensionless mean interfacial curvature, $\tilde{C}_m = C_m R$, where R is the largest inscribed circle in the cross section.

The geometry of the triangular capillary problem is presented in Figure A1. The first step in the solution is to determine L'/A. The cross-sectional perimeter of the gas-liquid and gas-solid interfaces, $L_{nw,w}$ and $L_{nw,s}$, and the area occupied by the nonwetting phase, A, are given below in terms of the geometrical parameters depicted in Figure A1:

$$L_{nw,w} = 3\omega a \qquad \text{(A2)}$$

$$L_{nw,s} = 6(\sqrt{3}R - a_1) \qquad \text{(A3)}$$

$$A = 3\sqrt{3}R^2 - 3aa_1\sin\left(\frac{\pi}{2} + \Psi\right) + \frac{3}{2}\omega a^2 \qquad \text{(A4)}$$

The first term in the expression for the area, Eq. A4, is the area of the entire triangle; the following two terms represent the area of the wetting liquid. Simple plane triangle geometry allows one to express ω in terms of the contact angle, Ψ, and a_1 in terms of Ψ and the interfacial radius of curvature a,

$$\omega = \frac{2\pi}{3} - 2\Psi \qquad \text{(A5)}$$

$$a_1 = 2a\sin\left(\frac{\pi}{3} - \Psi\right) \qquad \text{(A6)}$$

Equations A2 through A6 can be combined to give an expression for L'/A:

$$\frac{L'}{A} = \frac{2}{R}\left[\frac{3\sqrt{3}\cos\Psi + g(\Psi)\tilde{a}}{3\sqrt{3} + g(\Psi)\tilde{a}^2}\right] \qquad \text{(A7)}$$

where $g(\Psi) = \pi - 3\Psi - 6\cos\Psi\sin(\pi/3 - \Psi)$, and $\tilde{a} = a/R$.

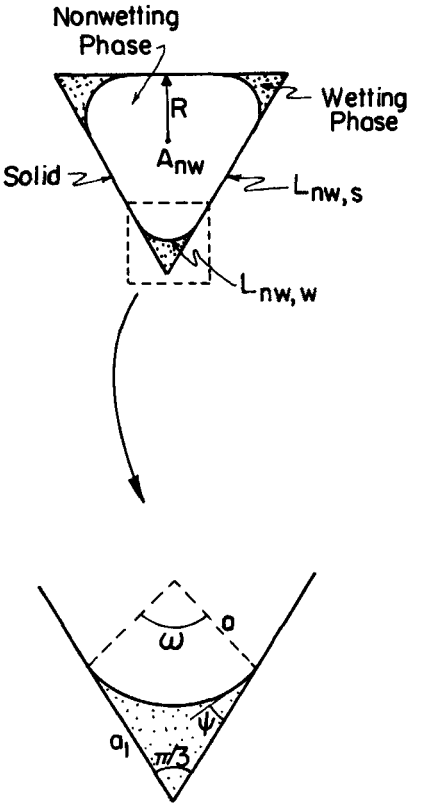

Figure A1. Geometry for calculation of minimum energy distribution of fluids at bubble front in an equilateral triangular capillary.

The minimum energy configuration is determined by minimizing L'/A for a given contact angle, Ψ, which is done by setting the derivative of the right side of Eq. A7 equal to zero,

$$\frac{d}{d\tilde{a}}\left[\frac{3\sqrt{3}\cos\Psi + g(\Psi)\tilde{a}}{3\sqrt{3} + g(\Psi)\tilde{a}^2}\right] = 0. \qquad \text{(A8)}$$

The differentiation indicated in Eq. A8 produces the quadratic expression shown below:

$$-g(\Psi)\tilde{a}^2 - 6\sqrt{3}\cos\Psi\tilde{a} + 3\sqrt{3} = 0. \qquad \text{(A9)}$$

Equation A9 can be solved for $\tilde{a}$,

$$\tilde{a} = \frac{3\sqrt{3}\cos\Psi \pm \sqrt{27\cos^2\Psi + 3\sqrt{3}g(\Psi)}}{-g(\Psi)}. \qquad \text{(A10)}$$

For the case where $\Psi = 0$, $\tilde{a}$ is calculated to be 0.564, and $\tilde{C}_m$, which is the inverse of $\tilde{a}$, is 1.77.

Literature cited

Adamson, A. W., *Physical Chemistry of Surfaces*, Wiley, New York, 509 (1976).

Arriola, A., G. P. Willhite, and D. W. Green, "Trapping of Oil Droplets in a Noncircular Pore Throat and Mobilization upon Contact with a Surfactant," *Soc. Pet. Eng. J.*, **23** (1), 99 (Feb., 1983).

Bretherton, F. P., "The Motion of Long Bubbles in Tubes," *J. Fluid Mech.*, **10**, 166 (1961).

Charpentier, J. C., and M. Favier, "Some Liquid Holdup Experimental Data in Trickle-Bed Reactors for Foaming and Nonfoaming Hydrocarbons," *AIChE J.*, **21** (6), 1213 (1975).
Clunie, J. S., J. F. Goodman, and B. T. Ingram, "Thin Liquid Films," *Surf. Colloid Sci.* **3**, 167 (1971).
Dullien, F. A. L., *Porous Media: Fluid Transport and Pore Structure*, Academic Press, New York, 88 (1979).
Fried, A. N., "The Foam-Drive Process for Increasing the Recovery of Oil," U.S. Dept. Interior, Bur. Mines, Rep. of Investigations 5866 (1961).
Gauglitz, P. A., "Instability of Liquid Films in Constricted Capillaries: A Pore-Level Description of Foam Generation in Porous Media," Ph.D. Thesis, Univ. California, Berkeley (1986).
Goren, S., "The Instability of an Annular Thread of Fluid," *J. Fluid Mech.*, **12**, 309 (1962).
Hammond, P. S., "Nonlinear Adjustment of a Thin Annular Film of Viscous Fluid Surrounding a Thread of Another within a Circular Cylindrical Pipe," *J. Fluid Mech.*, **137**, 363 (1983).
Legait, B., "Laminar Flow of Two Phases through a Capillary Tube with Variable Square Cross Section," *J. Coll. Interf. Sci.*, **96** (1), 28 (1983).
Lenormand, R., and C. Zarcone, "Role of Roughness and Edges During Imbibition in Square Capillaries," SPE 13264, 59th Ann. Meet. SPE, Houston (Sept., 1984).
Mast, R. F., "Microscopic Behavior of Foam in Porous Media," SPE 3997, 47th Ann. Fall Meet. SPE, San Antonio (Oct., 1972).
Mayer, R. P., and R. A. Stowe, "Mercury Porosimetry—Breakthrough Pressure for Penetration between Packed Spheres," *J. Coll. Interf. Sci.*, **20**, 893 (1965).
Mohanty, K. K., "Fluids in Porous Media: Two-Phase Distribution and Flow," Ph.D. Thesis, Univ. Minnesota (1981).
Ransohoff, T. C., "Foam Generation in Constricted Noncircular Capillaries and in Bead Packs," M.S. Thesis, Univ. California, Berkeley (1986).
Ransohoff, T. C., and C. J. Radke, "The Mechanisms of Foam Generation in Glass Bead Packs," SPE 15441, submitted to *SPE Reservoir Engineering* (1986a).
———, "Laminar Flow of a Wetting Liquid Along the Corners of a Predominantly Gas-Occupied Noncircular Pore," accepted *J. Coll. Interf. Sci.* (1986b).
Roof, J. G., "Snap-Off of Oil Droplets in Water-Wet Pores," *Soc. Pet. Eng. J.*, **10** (1), 85 (Mar., 1970).
Singhal, A. K., and W. H. Somerton, "Two-Phase Flow Through a Noncircular Capillary at Low Reynolds Numbers," 21st Ann. Tech. Meet. Petroleum Soc. CIM, Calgary (May, 1970).
Straus, A. E., W. A. Sweeney, R. House, and S. H. Sharman, "Foam Well Cleanout Using Oligomeric Sulfonates," U.S. Pat. No. 3,971,823 (Apr., 1976).

Manuscript received Jul. 17, 1986, and revision received Nov. 25, 1986.